Decisions in Economics and Finance
https://doi.org/10.1007/s10203-026-00600-w

A network analysis of systemic risk in the European banking sector

Alessandra Cornaro[1] · Edit Rroji[1] · Ilaria Stefani[2]

Received: 5 December 2025 / Accepted: 24 July 2026

Abstract

In this paper, we adopt a conditional tail risk network methodology for the assessment of transmission channels of risk. In particular, we employ weighted and directed networks to model the mutual influence between banks, with the weights being linked to tail risk measures. More specifically, in the empirical comparison we focus on MES-based pairwise dependence networks and on the parametric ΔCoVaR network estimated on ARMA(1,1)-GARCH(1,1) residuals through SCAD-penalized quantile regression. We use different network indicators to investigate the importance of a bank's role in both spreading and absorbing risk from other financial institutions. Our analysis focuses on a sample based on banks included in the European Banking Authority 2023 stress test, complemented by two additional systemically relevant European institutions and we consider daily data for the period 2015–2024. The analyses are conducted over four economically meaningful subperiods in order to evaluate the evolution of systemic interconnections across different macro-financial regimes. We find that the choice of tail risk measure leads to substantial differences in network topology, centrality rankings, and community composition. The empirical results demonstrate significant variations in the structural characteristics of the networks through time.

Keywords Network · Systemic risk · CoVaR · MES

JEL Classification C58 · G21 · G01 · D85

✉ Alessandra Cornaro
alessandra.cornaro@unimib.it

Edit Rroji
edit.rroji@unimib.it

Ilaria Stefani
ilaria.stefani@uni-ulm.de

1 Department of Statistics and Quantitative Methods, University of Milan-Bicocca, Piazza dell'Ateneo Nuovo 1, 20126 Milan, Italy

2 Institute of Insurance Science, Faculty of Mathematics and Economics, University of Ulm, Helmholtzstrasse 20, 89069 Ulm, Germany

Published online: 04 August 2026

1 Introduction

The resilience of financial systems has been extensively studied in the literature from multiple perspectives. For example, Kleinow and Moreira (2016) considered copula functions to address possible asymmetry in tail events, while Magner et al. (2021) suggested visualising the interconnectedness of banks using the minimum spanning tree computed on the correlation matrix. However, these approaches do not provide explicit insights into the contagion effect in the case of the failure of a single institution. A major breakthrough occurred with the paper by Adrian and Brunnermeier Adrian and Brunnermeier (2016), which focuses on the quantile of the system-wide distribution conditional on a given bank being in distress. This conditional quantile is called CoVaR, while the difference for two fixed confidence levels is called ΔCoVaR.

In the literature, most applications based on CoVaR refer to systemic risk measurement, see for example López-Espinosa et al. (2012), Pellegrini et al. (2022). In a multivariate framework, particular interest has been devoted to penalized regression for the CoVaR computation. In particular, Xu et al. (2019) use the LASSO method in CoVaR estimation to construct a systemic risk network among financial institutions' tail risk exposures by also considering lagged macroeconomics state variables. Following Ali et al. (2016) and Belloni et al. (2016), Torri et al. (2021) model conditional quantiles through smooth affine functions obtained with basis expansion, leading to the estimation of nonlinear quantile regression. More recently, Aprea et al. (2024) introduced a quantile Long Short-Term Memory network approach, which enables the simultaneous estimation of ΔCoVaR for various financial institutions. A different approach to systemic risk is presented in Fiori and Porro (2023), where a Compositional Data methodology is proposed to analyze the distribution of systemic risk contributions from major European countries between 2008 and 2021.

In this paper, we analyze the European banking system by means of a directed weighted network in which nodes represent banks and arc weights are defined using market-based measures. The methodology is related to that proposed in Clemente et al. (2020), where the Marginal Expected Shortfall (MES), introduced by Acharya et al. (2017), is computed pairwise to construct bilateral arcs and applied in Clemente and Cornaro (2022) to weight each network arc in a pool of insurance companies. The Marginal Expected Shortfall can be an effective indicator of systemic risk as highlighted in Idier et al. (2014). The literature on systemic risk and financial network analysis has expanded considerably over the past decade, covering a broad spectrum of approaches ranging from conditional tail-risk measures to contagion networks and capital-based systemic indicators. Pellegrini Pellegrini et al. (2022) examine how institutional characteristics are related to systemic risk using the CoVaR measure of Adrian and Brunnermeier (2016), documenting that systemic risk increases significantly with the size of large financial institutions. Abduraimova Abduraimova (2022) propose contagion measures based on copula theory, heavy-tailed distributions and network representations to investigate international stock market contagion during the 2008 global financial crisis, showing that shocks propagated predominantly from core to peripheral markets. Our analysis is also related to alternative systemic risk measures such as SRISK Brownlees and Engle (2017), which focuses on expected capital shortfall under systemic stress scenarios, and to high-frequency network-based systemic risk contributions (Hautsch et al. 2015), which capture short-term spillover dynamics through intraday return interactions. While these approaches provide valuable insights into solvency risk or short-run spillover intensity, they do not explicitly compare alternative tail-risk-based network constructions within a unified time-varying empirical framework. In contrast, our framework emphasizes tail-dependence-driven network topology and the evolution of community structures across distinct macro-financial regimes. To our knowledge, a systematic comparison between graphical quantile ΔCoVaR networks and MES-based bilateral networks within the same time-varying empirical setting remains largely unexplored.

The paper is positioned at the intersection of two strands of the literature. On the one hand, studies based on ΔCoVaR and quantile-network methods, such as Xu et al. (2019) and Torri et al. (2021), focus on directional tail dependence captured through conditional quantile structures. On the other hand, MES-based network approaches, such as Clemente et al. (2020) and Clemente and Cornaro (2022), construct bilateral links from conditional expected shortfall measures. Existing contributions typically analyse one of these two network families at a time. Our contribution is to compare the resulting network structures within the same empirical design, thereby showing how alternative tail-risk measures translate into different representations of systemic interconnectedness.

Our contribution is empirical and comparative rather than the introduction of a new systemic risk measure. We construct MES-based and ΔCoVaR-based banking networks on the same sample, over the same four subperiods, and analyse them through the same network indicators, so as to isolate how the choice of tail-risk measure affects the inferred structure of systemic interconnectedness. Within this unified framework, we compare network topology, centrality rankings, clustering patterns, and community composition, and we also relate network-based systemic importance to CDS-implied default probabilities in order to distinguish systemic interconnectedness from idiosyncratic fragility. The analysis is conducted over four economically meaningful subperiods, allowing us to assess the stability and reconfiguration of systemic interconnections under heterogeneous macro-financial regimes. In this sense, the paper should be viewed as a comparative empirical benchmark study of market-based systemic risk networks within a common setting rather than as a stand-alone methodological innovation. The empirical design is constructed so as to remain comparable with the closely related contribution of Torri et al. (2021), while extending the analysis to a more recent period characterized by major macro-financial events affecting the European banking system, including the Russian invasion of Ukraine and the subsequent inflationary phase observed in European markets. At the same time, since the methodology adopted in the paper is market-based and relies on daily equity returns, the empirical sample cannot coincide mechanically with the full European Banking Authority (EBA) stress-test universe, which also includes non-listed institutions. For this reason, the final sample should be interpreted as the market-observable subset of the relevant regulatory universe rather than as an arbitrary selection of banks. The paper is organized as follows.

In Sect. 2 we review the definition of conditional tail risk measures. In Sect. 3 we present some indicators for assessing the relevance of the financial institutions in the system and we model the financial system as a directed and weighted network. In

Sect. 4 we discuss the results of the empirical analyses while Sect. 5 concludes the paper.

2 Conditional tail risk measures

Here we discuss the two measures used in the paper as the main building blocks for network construction, namely ΔCoVaR and MES. Marginal Expected Shortfall is computed using a historical approach applied to daily returns, while for ΔCoVaR we consider three alternative specifications: a non-parametric version based on returns, a non-parametric version based on ARMA(1, 1)-GARCH(1, 1) residuals, and a parametric version based on the same residuals. [1]

The ARMA(1,1)-GARCH(1,1) filtering step is introduced to isolate cross-sectional tail dependence from time-series persistence in returns. Financial equity returns typically exhibit serial correlation in the conditional mean and volatility clustering in the conditional variance. If left untreated, these features may contaminate the estimation of cross-sectional tail dependence by inducing spurious dependence driven by common volatility dynamics rather than genuine inter-institutional effects.

2.1 Conditional value at risk

One of the most popular measures to identify systemic risk is CoVaR, as defined in Adrian and Brunnermeier (2016), which represents the financial system's Conditional Value at Risk (VaR) conditioned on an institution experiencing distress. Specifically, it represents an institution's contribution to systemic risk defined as the difference between the CoVaR conditioned on the institution's distress and the CoVaR under median institution conditions. However, some interpretations suggest that ΔCoVaR

[1] We present the ARMA(1, 1)–GARCH(1, 1) filtering step using the notation of Torri et al. (2021). We do not interpret this specification as the model uniformly selected by information criteria for all banks and all sub-periods. Instead, we use it as a common baseline filter. More precisely, given the time t realization of the random variable Y_i, the model ARMA(1, 1)−GARCH(1, 1) is specified as:

$$Y_{i,t} = \mu_{i,t} + \sqrt{h_{i,t}} I_{i,t}, \tag{1}$$

where $\mu_{i,t}$ is the t-realization of the conditional mean, $h_{i,t}$ the conditional variance and $I_{i,t}$ the standardized innovation. The innovations are assumed to be i.i.d. normally distributed. The dynamics for $\mu_{i,t}$ and $h_{i,t}$ are expressed in the following form:

$$\mu_{i,t} = c_i + \phi_i Y_{i,t-1} + \theta_i (Y_{i,t-1} - \mu_{i,t-1}), \tag{2}$$

$$h_{i,t} = \omega_i + \gamma_i h_{i,t-1} + \alpha_i (Y_{i,t-1} - \mu_{i,t-1})^2. \tag{3}$$

Model parameters are estimated using the **rugarch** package within the R programming environment, employing a maximum likelihood estimation procedure. Note that the framework could be extended by considering higher orders for the ARMA and/or the GARCH component or by fitting ARMA-(Exponential) GARCH models as done for example in Bellini et al. (2020) for the dynamics of the S&P500 and for the VIX indices. The residuals of these models can still be used as input of the parametric quantile graphical model under the Gaussian working specification used for the parametric construction; the adequacy of the retained filter is assessed through bank-level residual diagnostics reported in the Appendix.

is a measure of *systematic* risk rather than *systemic* risk, as it disregards the interconnectedness component found in many systemic risk definitions, focusing solely on the relationship between an institution and the entire market, as explained in Benoit et al. (2016). This observation motivates the adoption of a network-based conditional formulation, which explicitly incorporates pairwise interdependence across institutions. Using quantile graphical models, Torri et al. (2021) extend the approach to a network dimension, allowing us to examine the impact of the distress of one bank on the tail risk of all other banks in the system. This network extension of CoVaR, as originally outlined in Adrian and Brunnermeier (2016), suggests creating a network where each node corresponds to the ΔCoVaR of a pair of banks. However, it is important to note that this approach captures the unconditional effect on the tails. In contrast, quantile graphical models allow us to construct a network that captures the conditional effect on tails, namely the impact of an idiosyncratic shock to one bank on the rest of the system.

In its original formulation, CoVaR is defined as the quantile of the distribution of one firm's returns conditional on another firm being in distress. CoVaR is typically computed with respect to the entire market, conditioned on the stock returns of an entity being equal to their Value at Risk (VaR) at confidence level α, as in Adrian and Brunnermeier (2016). Following Torri et al. (2021), we extend the approach to the multivariate context, considering an n-variate distribution of returns. More precisely, we measure the quantile of the return distribution of bank i, conditional on institution j being in distress and on all the other institutions in the system being in their normal state, represented by the median case. Formally, we have

$$\Pr\left\{R_i \leq \mathrm{CoVaR}_\alpha^{R_i|R_j} \;\middle|\; R_j = \mathrm{VaR}_\alpha^{R_j},\; R_{\setminus\{i,j\}} = \mathrm{VaR}_{0.5}^{R_{\setminus\{i,j\}}}\right\} = \alpha, \tag{4}$$

where $R = (R_1, \ldots, R_n)^\top$ is an $\mathbb{R}^n$-valued random vector defined on a probability space $(\Omega, \mathcal{F}, \mathbb{P})$, R_i denotes the return random variable of institution i, and $R_{\setminus\{i,j\}}$ is the $(n-2)$-dimensional subvector collecting the returns of all institutions except i and j. The quantity $\mathrm{VaR}_{0.5}^{R_{\setminus\{i,j\}}}$ denotes the vector of componentwise median VaR levels for those institutions.

The equality

$$R_{\setminus\{i,j\}} = \mathrm{VaR}_{0.5}^{R_{\setminus\{i,j\}}}$$

is intended componentwise, i.e. each component of the subvector $R_{\setminus\{i,j\}}$ is fixed at its own median VaR level. It then follows that

$$\mathrm{CoVaR}_\alpha^{R_i|R_j} := \mathrm{VaR}_\alpha\left(R_i \;\middle|\; R_j = \mathrm{VaR}_\alpha^{R_j},\; R_{\setminus\{i,j\}} = \mathrm{VaR}_{0.5}^{R_{\setminus\{i,j\}}}\right).$$

After calculating $\mathrm{CoVaR}_\alpha^{R_i|R_j}$ for each pair of institutions, we obtain ΔCoVaR in the same way as in the bivariate case, by subtracting from $\mathrm{CoVaR}_\alpha^{R_i|R_j}$ the conditional quantile of R_i when all other institutions are in their median state. Specifically,

$$\Delta\mathrm{CoVaR}_\alpha^{R_i|R_j} := \mathrm{CoVaR}_\alpha^{R_i|R_j} - \mathrm{VaR}_\alpha\left(R_i \;\middle|\; R_j = \mathrm{VaR}_{0.5}^{R_j},\; R_{\setminus\{i,j\}} = \mathrm{VaR}_{0.5}^{R_{\setminus\{i,j\}}}\right). \tag{5}$$

To avoid ambiguity, we distinguish between $\bar{\alpha}$, the quantile level used in the conditional quantile network, and α, the tail probability entering VaR and CoVaR. In our empirical implementation, the network is estimated at $\bar{\alpha} = 0.5$, while α remains the distress level used in the risk measure. We first notice that we can express the conditional quantile of a random variable R_i given the others as

$$Q_{R_i,\bar{\alpha}} = f\left(R_{\setminus i}, \bar{\alpha}\right), \tag{6}$$

where f is a generic function and $R_{\setminus i}$ is the $(n-1)$-dimensional subvector obtained by removing the i-th component. Assuming an additive form of the conditional quantile function,

$$f\left(R_{\setminus i}, \bar{\alpha}\right) = \sum_{j \neq i} f_j\left(R_j, \bar{\alpha}\right),$$

it is possible to estimate quantile graphical models using linear or nonlinear quantile regression Koenker (1978). Following Ali et al. (2016) and Belloni et al. (2016), we model conditional quantiles through smooth affine functions obtained with basis expansion, leading to the estimation of nonlinear quantile regression. In this paper, we adopt an additive linear specification of the conditional quantile function:

$$f\left(R_{\setminus i}, \bar{\alpha}\right) = \eta_i + \sum_{j \neq i} \beta_{\bar{\alpha}}^{i|j} R_j,$$

where η_i is the intercept and $\beta_{\bar{\alpha}}^{i|j}$ is the regression coefficient. The quantile graphical framework enables the identification of directional conditional dependence in a multivariate setting. In particular, the coefficient $\beta_{\bar{\alpha}}^{i|j}$ measures the change in the conditional $\bar{\alpha}$-quantile of institution i associated with a one-unit increase in institution j, holding the returns of the other institutions fixed. Thus, $\beta_{\bar{\alpha}}^{i|j}$ quantifies how the conditional quantile of bank i reacts to variations in bank j within the network structure. When $\bar{\alpha}$ is chosen in the lower part of the distribution, this coefficient can be interpreted as capturing directional lower-tail dependence. In this paper, we consider penalized quantile regression, a method designed to improve the efficiency of the estimator, especially when dealing with many variables relative to the number of observations. In particular, we consider quantile regression with SCAD (Smoothly Clipped Absolute Deviation) penalization proposed by Wu and Liu (2009). Each quantile regression can be computed by minimizing

$$\begin{aligned} &\min_{\beta_{\bar{\alpha}}^{i|1},\ldots,\beta_{\bar{\alpha}}^{i|n}} \mathbb{E}\left[\rho_{\bar{\alpha}}\left(R_i - \sum_{j=1,\, j\neq i}^{n} \beta_{\bar{\alpha}}^{i|j} R_j\right)\right] \\ &+ \sum_{j=1,\, j\neq i}^{n} t\sqrt{\bar{\alpha}(1-\bar{\alpha})}\, p_\lambda(\beta_{\bar{\alpha}}^{i|j}), \qquad \forall i = 1, \ldots, n, \end{aligned} \tag{7}$$

where $\rho_{\bar{\alpha}}(r) = (\bar{\alpha} - \mathbb{I}_{r\leq 0})r$ is the asymmetric loss function, $\beta_{\bar{\alpha}}^{i|1}, \ldots, \beta_{\bar{\alpha}}^{i|n}$ are the regression coefficients, t is the number of observations and $p_\lambda(\beta)$ is the penalization function. The SCAD penalty defined in Fan and Li (2001) reads

$$p_\lambda^{SCAD}(\beta) = \begin{cases} \lambda|\beta| & \text{if } |\beta| \le \lambda, \\ -\dfrac{|\beta|^2 - 2a\lambda|\beta| + \lambda^2}{2(a-1)} & \text{if } \lambda < |\beta| \le a\lambda, \\ \dfrac{(a+1)\lambda^2}{2} & \text{if } |\beta| > a\lambda, \end{cases} \tag{8}$$

where λ and a are positive parameters. We adopt SCAD-penalized linear quantile regression to induce sparsity in the estimated cross-sectional tail dependence structure and to ensure stability in a high-dimensional setting. In our empirical design, a separate node-wise quantile regression is estimated for each institution and for each time window. In this context, sparsity is essential to avoid overfitting and to prevent the emergence of spurious links that would artificially inflate network density and distort centrality measures. In practice, the penalty parameter λ is selected through a BIC-type criterion evaluated over a finite grid of candidate values, and the value minimizing the information criterion is retained. The SCAD shape parameter a is fixed at 3.7 following Fan and Li (2001), as customary in empirical applications. Let $\beta_{0.5}^{i|\setminus i}$ denote the vector of coefficients in the multivariate penalized quantile regression of R_i on the remaining returns $R_{\setminus i}$ and let $\beta_{0.5}^{i|j}$ denote its j-th component. In our empirical implementation, the dependence structure is estimated through a conditional median network, namely by fixing the network quantile level at $\bar{\alpha} = 0.5$. This choice provides a stable benchmark representation of cross-sectional conditional dependence under ordinary market conditions, while the tail probability α is reserved for the distress event entering VaR and CoVaR. Moreover, under the Gaussian specification adopted for the parametric construction, the slope coefficients of the conditional quantile function do not depend on the quantile level. Therefore, the coefficients estimated in the conditional median network coincide with those associated with any other conditional quantile level, which justifies using $\beta_{0.5}^{i|j}$ as the building block for the parametric ΔCoVaR. Accordingly, in our empirical implementation, the historical-distribution-based variant of ΔCoVaR is computed as

$$\Delta\mathrm{CoVaR}_\alpha^{R_i|R_j} = \beta_{0.5}^{i|j}\left(\mathrm{VaR}_\alpha^{R_j} - \mathrm{VaR}_{0.5}^{R_j}\right). \tag{9}$$

Equation (9) corresponds to the implemented non-parametric ΔCoVaR, obtained by combining the coefficients of the conditional median network with historical VaR estimates. We now recall the formulation of the parametric ΔCoVaR following Torri et al. (2021), under the assumption that the returns R_i are centered and normally distributed. In this case,

$$\Delta\mathrm{CoVaR}_\alpha^{R_i|R_j} = \beta_{0.5}^{i|j}\,\Phi^{-1}(\alpha)\,\sigma(R_j), \tag{10}$$

where $\sigma(R_j)$ denotes the unconditional standard deviation of R_j and Φ is the cumulative distribution function of the standard normal distribution.

2.2 Marginal expected shortfall

We use Marginal Expected Shortfall (MES) as a measure of the tail influence of one bank on another. In a system with n banks, the Marginal Expected Shortfall of bank i is defined in Acharya et al. (2017) as a conditional expectation of returns. Here, focusing on pairs of banks, we define the Expected Shortfall of bank i conditional on bank j being in distress in the same period as

$$\mathrm{MES}_\alpha^{i|j} = -\mathbb{E}\Big(R_i \mid R_j \leq \mathrm{VaR}_\alpha^{R_j}\Big). \tag{11}$$

From (11), MES corresponds to the expected return of bank i conditional on the return of bank j falling below its Value-at-Risk at confidence level α (denoted by $\mathrm{VaR}_\alpha^{R_j}$). Following Clemente et al. (2020), rather than considering a bank relative to the entire system, we focus on bilateral relationships between banks i and j.

To evaluate the tail influence of bank j on bank i within the same window, we consider

$$\mathrm{ES}_\alpha^{i} - \mathrm{MES}_\alpha^{i|j} = -\mathbb{E}\Big(R_i \mid R_i \leq \mathrm{VaR}_\alpha^{R_i}\Big) + \mathbb{E}\Big(R_i \mid R_j \leq \mathrm{VaR}_\alpha^{R_j}\Big). \tag{12}$$

This quantity is non-negative and values closer to zero indicate a stronger tail impact of bank j on bank i. To ensure comparability across institutions, we scale this difference by the gap between the unconditional expected return $\mathbb{E}(R_i)$ and the tail expectation $\mathbb{E}(R_i \mid R_i \leq \mathrm{VaR}_\alpha^{R_i})$.

The impact of bank j on bank i in the same period is then defined as

$$I_{i|j} = \frac{-\mathbb{E}\Big(R_i \mid R_i \leq \mathrm{VaR}_\alpha^{R_i}\Big) + \mathbb{E}\Big(R_i \mid R_j \leq \mathrm{VaR}_\alpha^{R_j}\Big)}{\mathbb{E}(R_i) - \mathbb{E}\Big(R_i \mid R_i \leq \mathrm{VaR}_\alpha^{R_i}\Big)}. \tag{13}$$

The quantity $I_{i|j}$ is non-negative since both numerator and denominator are non-negative. Moreover, when $\mathbb{E}(R_i) < \mathbb{E}(R_i \mid R_j \leq \mathrm{VaR}_\alpha^{R_j})$, we observe a positive reaction of i to the distress of bank j. As our primary focus is systemic risk, we disregard such favorable effects and constrain $I_{i|j}$ to the interval [0, 1]. The denominator captures the overall individual downside risk of bank i, so $I_{i|j}$ measures the fraction of this risk not attributable to bank j. Specifically, a value of $I_{i|j}$ close to zero suggests that the risk of bank i is significantly influenced by bank j.

3 Networks

3.1 Preliminary definitions and notations

In this section, we briefly recall some mathematical definitions and notations used in the paper (for further details we refer to Bang-Jensen and Gutin (2009) and Harary (1969)). A graph $G = (V, E)$ is identified by a set V of n vertices and a set E of m unordered edges. Vertices i and j are adjacent (or neighbours) if the edge $e_{i,j} \in E$.

A path between two vertices i and j is defined as a sequence of distinct vertices and edges between i and j, indicating that i and j are connected. The graph G is connected if every pair of vertices is connected. A shortest path between two vertices is a path with the minimum number of edges and it is called geodesic.

The distance $d_{i,j}$ represents the length of any shortest path between vertices i and j. If i and j are not connected, then $d_{i,j} = \infty$. The diameter $diam(G)$ of a connected graph is the length of any longest shortest path.

A graph G is weighted when a positive real number $w_{i,j} > 0$ is associated with the edge $e_{i,j}$. In cases where vertices i and j are not adjacent, the weight is set to $w_{i,j} = 0$. In the context of weighted graphs, a shortest path is defined as a path with the minimum sum of edge weights. This means that the total weight of the path is minimized. For weighted graphs, a weighted distance, denoted as $d_{i,j}^W$, can be defined as the sum of weights of the shortest path between vertices i and j. If vertices i and j are not connected, then $d_{i,j}^W$ is set to ∞, similar to the unweighted case.

The weighted adjacency matrix, denoted as $\mathbf{W}$, is an $n \times n$ real non-negative matrix that describes the adjacency relationships between vertices of graph G and the weights on the edges. The entries of this matrix are represented as $w_{i,j}$. In the unweighted case, matrix $\mathbf{W}$ is simply the classical binary matrix $\mathbf{A}$, the so-called adjacency matrix. In what follows, we consider both unweighted and weighted graphs with no loops (i.e. $a_{i,i} = 0$, $w_{i,i} = 0 \ \forall i$). A directed graph $D = (V, E)$ is derived from graph G by assigning a direction to its edges. Graph G serves as the underlying graph of D. In this context, the connections between pairs of vertices are referred to as arcs or directed edges. Additionally, each arc $e_{i,j}$ is associated with a weight $w_{i,j}$, where $w_{i,j} > 0$. It is noteworthy that the matrix $\mathbf{W}$ may not be symmetric, as distinct arcs between a pair of vertices can result in different weights. This means that both $w_{i,j}$ and $w_{j,i}$ can be positive, and in general, $w_{i,j} \neq w_{j,i}$ due to the existence of two distinct arcs between the same pair of vertices. A directed path from i to j is a sequence of distinct vertices and arcs from i to j such that every arc has the same direction. In this case, we say that j is reachable from i, and we define this directed path as the out-path of the vertex i. The distance $\overrightarrow{d_{i,j}}$ from i to j is the length of the shortest out-path, if any; otherwise, $\overrightarrow{d_{i,j}} = \infty$. Similarly, directed paths from j to i can also exist. We denote the length of the shortest in-path of the vertex i based on the directed path from j to i as $\overleftarrow{d_{i,j}}$. If i is not reachable from j, then $\overleftarrow{d_{i,j}} = \infty$.

D is strongly connected if every two vertices are mutually reachable. D is weakly connected if the underlying graph G is connected. Weighted directed distances $\overleftarrow{d_{i,j}^W}$ and $\overrightarrow{d_{i,j}^W}$ can also be defined as the sum of the weights of the weighted directed shortest paths.

3.2 Network indicators

In order to identify the most significant banks and assess contagion risk, we make use of suitable local network indicators. Given the high interconnectedness of the system, the risk of a single bank affects all other banks, and no bank can be immune to contagion if another bank is distressed. The indicators are able to capture some relevant aspects of contagion, including the local level of interconnection and the dominant position of a bank in the system in terms of spreading or receiving risk.

3.2.1 Classical centrality measures

In network analysis, centrality is a key concept that focuses on identifying important elements within a network's structure. These elements can include vertices, edges, or groups of vertices, and their importance is often assessed in terms of their overall impact on the network. While various aspects of centrality are studied, the assignment of a centrality score to individual vertices is a widely explored topic. In the past decades, a variety of measures have been introduced to pursue this aim. In what follows, we focus on the most well-known and commonly used measures, particularly in their weighted versions.

One of the most intuitive centrality measures is the degree centrality of a vertex, d_i, which counts the number of vertices adjacent to vertex i. For a directed graph, we can define the in-degree of a node i, denoted by d_i^{in}, as the number of arcs that point towards i and the out-degree d_i^{out} of a node i as the number of arcs that start from i. The degree, denoted by d_i^{tot}, of a vertex is the sum of the in-degree and out-degree. Finally, the degree of bilateral arcs between node i and its adjacent nodes is expressed as $d_i^{\leftrightarrow} = \sum_{j \neq i} a_{ij} a_{ji} = \sum_{j \neq i} a_{i,j} a_{j,i}$, where $a_{i,j}$ is equal to 1 if i and j are adjacent nodes and to 0 otherwise. For a weighted graph, we can calculate the strength by defining it as $s_i = \sum_{j=1}^{n} w_{i,j}$, where $w_{i,j}$ represents the weights. These strength values can then be collected in a vector $s = (s_1, ..., s_n)^\top$. For a weighted and directed graph with weighted adjacency matrix $\mathbf{W} = (w_{ij})_{i,j=1}^{n}$, the in-strength of vertex i is defined as

$$s_i^{\text{in}} = \sum_{j \neq i} w_{ji}, \tag{14}$$

while the out-strength is given by

$$s_i^{\text{out}} = \sum_{j \neq i} w_{ij}. \tag{15}$$

The total strength of vertex i is therefore defined as the sum of its in- and out-strength:

$$s_i^{\text{tot}} = s_i^{\text{in}} + s_i^{\text{out}} = \sum_{j \neq i} \left(w_{ij} + w_{ji} \right). \tag{16}$$

Finally, the strength associated with bilateral arcs between node i and its adjacent nodes can be written as

$$s_i^{\leftrightarrow} = \frac{1}{2} \sum_{j \neq i} \left(w_{ij} a_{ji} + w_{ji} a_{ij} \right), \tag{17}$$

where a_{ij} denotes the (i, j) element of the binary adjacency matrix $\mathbf{A}$.

3.2.2 Hubs and Authorities

To better capture the significance of a vertex within a network, we adopt centrality measures. In particular, the most appropriate measure for this purpose is the eigenvector centrality, which can be extended to weighted and directed networks. In the context of an undirected graph, the eigenvector centrality of a given vertex i corresponds to the i-th component of the eigenvector associated with the maximum eigenvalue of the (weighted) adjacency matrix (refer to Horn and Johnson (2012) for further details).

In the extension of this measure to directed networks, a vertex is associated with two scores: authority and hubness. This concept is particularly relevant in the context of web page search, as it is used to rank the importance of a page (see Kleinberg (1999a) and Kleinberg (1999b)). In this context, a web page is considered an authority when many other pages point to it, while hubs are pages that link to many authoritative pages.

Let x_i and y_i be the authority and hub scores of vertex i, respectively. These scores satisfy the following relations:

$$x_i = \sum_{j \neq i} w_{ji} y_j, \tag{18}$$

and

$$y_i = \sum_{j \neq i} w_{ij} x_j. \tag{19}$$

In the realm of web analysis, hubs and authorities are defined by a mutually reinforcing relationship. A good hub is a page that points to many good authorities, while a good authority is a page to which many good hubs point.

The iterative algorithm proposed for computing the scores is known as HITS (Hyperlink-Induced Topic Search), which was introduced by Kleinberg (1999a).

In our framework, this double-score is interpreted as follows. A bank that has a high authority score is expected to be highly influenced in terms of its risk by the neighbouring bank's risk. In contrast, banks that have high hub scores are dominant in risk diffusion and, thus, affect many neighbours.

3.2.3 Clustering coefficient

In network theory, the clustering coefficient is a measure of the degree to which nodes in a graph tend to cluster together. This measure provides insights into the structure of networks, particularly social networks, where nodes tend to form tightly knit groups characterized by a relatively high density of ties. In this work we focus on the local clustering coefficient for weighted and directed networks, as introduced by Fagiolo in Fagiolo (2007), that describes the tendency of a network to form highly connected groups of nodes. The work of Clemente and Grassi (2018) extended this clustering coefficient, offering a new perspective for assessing local clustering in complex networks, with a specific focus on weighted and directed networks and providing a more detailed analysis of the clustering structure within such networks. We present here all the formulations implemented in the empirical analysis.

The local clustering coefficient of a node i in a graph is a measure of the likelihood that the neighbors of node i are also connected to each other. It is calculated by dividing the number of actual weighted directed triangles connected to node i by its total number of potential unweighted directed triangles. The overall clustering coefficient provided by Fagiolo is defined as follows:

$$C_i^{\mathrm{F}}(\tilde{\mathbf{W}}) = \frac{\frac{1}{2}\left[\left(\tilde{\mathbf{W}}^{[1/3]} + \left(\tilde{\mathbf{W}}^{\top}\right)^{[1/3]}\right)^3\right]_{ii}}{d_i^{tot}(d_i^{tot}-1) - 2d_i^{\leftrightarrow}}, \tag{20}$$

where $\tilde{\mathbf{W}} = [\tilde{w}_{i,j}]_{i,j\in V}$ is the normalized weighted matrix whose elements are defined as $\tilde{w}_{i,j} = \frac{w_{i,j}}{\max_{i,j} w_{i,j}}$.

In this framework, in-clustering and out-clustering coefficients may be more suitable for capturing how risk propagates from a node to its adjacent nodes. They are defined as follows:

$$C_i^{\mathrm{F}in}(\tilde{\mathbf{W}}) = \frac{\frac{1}{2}(\tilde{\mathbf{W}}^{\top}\tilde{\mathbf{W}}^2)_{ii}}{d_i^{in}(d_i^{in}-1)} \tag{21}$$

$$C_i^{\mathrm{F}out}(\tilde{\mathbf{W}}) = \frac{\frac{1}{2}(\tilde{\mathbf{W}}^2\tilde{\mathbf{W}}^{\top})_{ii}}{d_i^{out}(d_i^{out}-1)}. \tag{22}$$

We now present the overall coefficient provided by Clemente and Grassi in Clemente and Grassi (2018):

$$C_i^{\mathrm{BCG}}(\mathbf{W}) = \frac{\frac{1}{2}\left[(\mathbf{W}+\mathbf{W}^{\top})(\mathbf{A}+\mathbf{A}^{\top})^2\right]_{ii}}{s_i^{tot}(d_i^{tot}-1) - 2s_i^{\leftrightarrow}}. \tag{23}$$

It is possible to specify a directed clustering coefficient in order to have coefficients taking into account the different patterns. Each coefficient is defined as the number of actual specific triangles of i divided by the number of potential specific triangles of i, giving information about the clustering of the nodes with respect to the pattern in which they are involved. For the in-component we have:

$$C_i^{\mathrm{BCG}\,in}(\mathbf{W}) = \frac{\frac{1}{2}\left[\mathbf{W}^\top(\mathbf{A}+\mathbf{A}^\top)\mathbf{A}\right]_{ii}}{s_i^{in}(d_i^{in}-1)} \tag{24}$$

and for the out-component:

$$C_i^{\mathrm{BCG}\,out}(\mathbf{W}) = \frac{\frac{1}{2}\left[\mathbf{W}(\mathbf{A}+\mathbf{A}^\top)\mathbf{A}^\top\right]_{ii}}{s_i^{out}(d_i^{out}-1)}. \tag{25}$$

The arc from node i to node j represents the influence, in terms of risk, of bank i on bank j. This bilateral relationship assumes that a bank's distress not only affects but is also impacted by the distress of all its neighboring banks. The intensity of this influence is measured by using $w_{i,j}$. Each bank, represented by i, participates in two distinct types of triangles within the network: the in-type and the out-type. In the in-type triangle, bank i is influenced by both of its adjacent nodes, j and k. On the other hand, in the out-type triangle, bank i propagates risk to its adjacent nodes. This dynamic interplay within the banking network highlights the interconnected nature of risk and influence among the participating banks.

3.3 Community detection

One key aspect of network analysis is the identification of community structures, which represent cohesive groups of nodes within a network. In this framework, community detection plays a crucial role in uncovering the underlying structure and organization of the network. The community configurations reported in the empirical analysis should be interpreted primarily as reflecting patterns of tail dependence among banks' returns. At the same time, other factors such as geographical proximity, similarities in business models, and the composition of the empirical sample may also contribute to the observed clustering. For this reason, the discussion of community structures is intended as an interpretation of the network output rather than as a causal attribution to a single economic mechanism. To this end, we apply a well-known community detection method, the Walktrap algorithm. The Walktrap algorithm (see Pons and Latapy (2006)) is based on the concept of random walks within the network. The rationale behind the algorithm is that nodes within the same community are likely to be visited by random walks more frequently than nodes from different communities. By measuring the similarities between nodes based on the random walk process, the algorithm can identify cohesive groups of nodes, representing communities within the network. This behavior forms the basis for the algorithm's ability to identify and merge communities based on the results of these random walks. A pivotal aspect of the Walktrap algorithm lies in its algorithmic framework, which involves the iterative exploration of network neighborhoods through random walks and the subsequent measurement of node similarity based on the paths traversed. This method encompasses several steps with the aim to unveil community structures. In particular, the algorithm involves the construction of a similarity matrix based on a measure of similarity between vertices derived from random walks. This matrix captures the community structure in the network efficiently and forms a foundational component of the algorithm's operations. Following the construction of the similarity matrix, the algorithm calculates pairwise node distances. This step is crucial for understanding the relationships and distances between nodes within the network. The final procedural step involves the hierarchical clustering of nodes to unveil community structures within the network. This process allows for the identification of densely connected subnetworks, or communities, through the utilization of the similarity matrix and pairwise node distances. One of the key advantages of the Walktrap algorithm is its ability to detect communities of varying sizes and shapes, making it suitable for a wide range of network structures. Additionally, the algorithm is computationally efficient.

3.4 Building the financial network

Our goal is to construct a risk network tailored to capture interdependencies between banks through the market-based risk measures introduced in Sect. 2. More specifically, we aim to quantify the effect of the distress of one institution on the risk profile of the others, consistently with the notion of systemic risk. To this end, we model the financial system as a directed and weighted network in which vertices represent banks and arc weights are determined by pairwise tail-risk measures. This framework allows us to investigate the role of each institution in the system, both in terms of spreading and receiving risk.

In the network representation we adopt the usual graph convention that the arc (i, j) is directed from the source institution i to the affected institution j. Therefore, the network weight $w_{i,j}$ is constructed from the pairwise contribution of bank i to bank j. We first consider a directed and weighted network, denoted by $G_{\Delta\text{CoVaR}}$, whose vertices are banks and where each arc $e_{i,j} \in E_t$, with $i \neq j$, is assigned a positive weight corresponding to the impact of bank i on bank j. Since, by definition, $\Delta\text{CoVaR}_\alpha^{R_j|R_i}$ measures the effect of institution i on institution j, the arc weights are defined as

$$w_{i,j}^{\Delta\text{CoVaR}} = \begin{cases} \Delta\text{CoVaR}_\alpha^{R_j|R_i}, & \text{if } i \neq j \text{ and } \Delta\text{CoVaR}_\alpha^{R_j|R_i} > 0, \\ 0, & \text{otherwise.} \end{cases} \tag{26}$$

Accordingly, an arc from node i to node j is interpreted as a directional spillover from institution i to institution j.

For $G_{\Delta\text{CoVaR}}$, the adjacency relations between pairs of vertices are represented by the real non-negative matrix $\mathbf{W}_{\Delta\text{CoVaR}}$, whose generic entry is $w_{i,j}^{\Delta\text{CoVaR}}$. This matrix serves as the weighted adjacency matrix of the network. Since our objective is to capture adverse systemic spillovers, we retain only the positive part of ΔCoVaR in the network construction. This guarantees non-negative edge weights and preserves the standard interpretation of centrality, clustering, and community-detection measures in weighted directed networks.

We construct three variants of the ΔCoVaR network, corresponding to the three specifications discussed in Sect. 2: non-parametric using raw returns, non-parametric using ARMA(1, 1)-GARCH(1, 1) residuals, and parametric using the same residuals.

In order to assess whether the dependence structure obtained from alternative tail-risk measures provides different information on systemic risk transmission and bank fragility, we also construct a network based on Expected Shortfall and Marginal Expected Shortfall (MES), following Clemente et al. (2020) and Clemente and Cornaro (2022). This second network, denoted by G_{MES}, is built on the same set of vertices and uses arc weights derived from the bilateral MES-based impact measure.

Recall that $I_{i|j}$ measures the impact of bank j on bank i as in formula (13), that is, the fraction of the downside risk of institution i that is not attributable to institution j. Accordingly, $1 - I_{i|j}$ captures the portion of downside risk of institution i associated with the distress of institution j. Hence, in order to assign to the arc (i, j) the impact of bank i on bank j, we use $1 - I_{j|i}$ and we define the MES-based weights as:

$$w_{i,j}^{\text{MES}} = \begin{cases} 1 - I_{j|i}, & \text{if } i \neq j \text{ and } \mathbb{E}(R_j) \geq \mathbb{E}(R_j \mid R_i \leq \text{VaR}_\alpha^{R_i}), \\ 0, & \text{otherwise.} \end{cases} \tag{27}$$

Also in this case, the arc (i, j) represents the impact of institution i on institution j.

For G_{MES}, the adjacency relations between pairs of vertices are represented by the matrix $\mathbf{W}_{\text{MES}}$, whose entries are $w_{i,j}^{\text{MES}}$. A larger value of $w_{i,j}^{\text{MES}}$ indicates a stronger tail effect of bank i on bank j, while a lower value indicates a weaker bilateral dependence. In particular, when $w_{i,j}^{\text{MES}}$ is close to one, the distress of bank i explains a large portion of the downside risk of bank j.

Therefore, both $G_{\Delta\text{CoVaR}}$ and G_{MES} are directed weighted networks defined on the same set of banks and observed over the same time windows. The only difference lies in the way pairwise spillovers are quantified: conditional quantile effects in the case of ΔCoVaR, and conditional tail expectations in the case of MES.

4 Empirical analysis

The empirical analysis is designed to remain comparable with the closely related contribution of Torri et al. (2021), while extending the analysis to a more recent period characterized by major macro-financial events affecting the European banking system, including the Russian invasion of Ukraine and the subsequent inflationary phase observed in European markets. At the same time, our empirical design is anchored to the EBA 2023 stress test universe, which provides the relevant regulatory reference set. However, the EBA stress test is defined for supervisory purposes and therefore includes institutions that are systemically relevant from a regulatory perspective, irrespective of whether they are publicly listed or continuously observable through market prices. By contrast, the construction of both MES- and ΔCoVaR-based networks requires market-based variables, in particular daily equity returns, and therefore can only be implemented for institutions for which these data are available over the full sample period. For this reason, the final empirical sample should not be interpreted as an arbitrary subset of the EBA universe, but rather as the market observable subset of that universe for which a consistent market-based network analysis is feasible. The sample is admittedly unbalanced across countries in a descriptive sense, but this imbalance reflects differences in listing structures, market liquidity, and data availability across national banking systems, rather than discretionary sample selection. More specifically, institutions that are not publicly listed are excluded, since the network measures employed in the paper rely on daily equity-return data. Among listed institutions, we retain only those for which daily equity returns are available over the period 11/19/2015–03/08/2024. We further exclude institutions whose equity series display insufficient market liquidity, since sparse trading may generate unstable return dynamics and distort the estimation of tail-risk dependence. Finally, for the part of the empirical analysis involving CDS-implied default probabilities, we retain only institutions for which consistent five-year default-probability data are available. Under these criteria, 34 institutions from the EBA 2023 stress test list are included in the baseline empirical sample. In addition, we consider two large non-EU institutions, HSBC Holdings plc and UBS, because of their systemic relevance within the broader European financial landscape and the availability of the required market-based variables, yielding a final sample of 36 institutions. Table 1 reports the full list of the EBA institutions included in the empirical sample. The community results are interpreted in light of the empirical design and the sample-construction criteria adopted in the analysis. Given the empirical sample, we investigate the transmission of systemic risk within the banking sector. We replicate our analysis for sub-windows of periods that we consider historically relevant, such as Brexit, the COVID-19 pandemic crisis, post-COVID high inflation and recent international conflicts, with the aim of understanding the dynamics that are important for the transmission of systemic risk in different economic scenarios. The four time windows considered are (a) 11/19/2015 to 12/31/2017, (b) 01/01/2018 to 02/15/2020, (c) 02/16/2020 to 01/31/2022 and (d) 02/01/2022 to 03/08/2024. The data set covers periods of low and high interest rates that have impacted the perceived risk in the financial system.

In practice, we construct a directed weighted network in each period. For each time window, we estimate VaR and ES for each bank, and pairwise CoVaR and MES measures for each ordered pair of institutions for $\alpha = 0.05$. From now on, we will omit α in the definition of various risk measures. In particular, for each of the four time windows, we have constructed a sequence of directed and weighted networks, where the banks are the vertices and the weights of the arcs are related to the impact between institutions. Note that, since the number of banks does not vary over time, we refer to the number assigned to each institution in Table 1. From the same table, it can be seen that the largest standard deviation of returns over the period under consideration comes from Greek banks, but only one of them (National Bank of Greece SA) has a high probability of default at the end of the period.

Networks for the four time windows where weights are computed using MES are presented in Fig. 1 while Fig. 2 displays the networks based on the parametric

Table 1 List of banks considered in the analysis. For each institution, we provide the first four moments of daily returns computed on the time window from 11/19/2015 to 03/08/2024. The last column refers to the 5-year default probability (P^D) as downloaded from Bloomberg on 03/20/2024

Institution	Short name	Country	Mean	Dev.st	Skew	Kurt	P^D
1. Commerzbank AG	COMMERZ	Germany	−2.63E-05	0.026	0.199	4.820	0.089
2. Erste Group Bank AG	ERSTE	Austria	−1.30E-04	0.021	0.276	7.583	0.101
3. Raiffeisen Bank International AG	RAIFF	Austria	−9.17E-05	0.023	0.910	12.990	0.122
4. KBC Group NV	KBC	Belgium	−9.61E-05	0.021	1.058	12.979	<0.01
5. ABN AMRO Bank NV	ABN	Netherlands	8.50E-05	0.022	1.022	12.759	0.081
6. ING Groep NV	ING	Netherlands	−1.22E-05	0.022	0.587	13.202	0.114
7. Credit Agricole Groupe	CR AGR	France	−5.20E-05	0.020	0.780	11.755	0.110
8. BNP Paribas SA/Taipei	BNP	France	−2.13E-05	0.021	0.679	9.911	0.109
9. HSBC Holding PLC	HSBC	UK	4.88E-05	0.017	0.164	4.948	0.099
10. Barclays Bank PLC	BARCL	Ireland	1.33E-04	0.022	0.798	11.460	0.179

Table 1 continued

Institution	Short name	Country	Mean	Dev.st	Skew	Kurt	P^D
11. Skandinaviska Enskilda Banken AB	SK.VISCA	Sweden	−1.54E-04	0.018	1.103	9.267	0.102
12. Swedbank AB	SWED	Sweden	1.20E-05	0.018	1.488	10.963	0.098
13. Svenska Handelsbanken AB	SV.HB	Sweden	5.34E-05	0.017	0.810	7.441	0.072
14. DNB Bank ASA	DNB	Norway	−1.87E-04	0.019	0.786	8.979	< 0.01
15. Bank Polska Kasa Opieki SA	BPKO	Poland	−8.28E-05	0.023	0.649	11.458	0.190
16. Danske Bank A/S	DANSKE	Denmark	−3.20E-05	0.018	0.299	4.722	0.061
17. Jyske Bank A/S	JYSKE	Denmark	−2.46E-04	0.018	−0.050	6.973	<0.01
18. Sydbank AS	SYD	Denmark	−2.40E-04	0.019	0.695	9.390	< 0.01
19. Nordea Bank Abp	NORDEA	Finland	−3.75E-05	0.017	1.006	7.901	0.054
20. Alpha services & Holdings SA	ALPHA	Greece	2.49E-04	0.036	0.701	11.143	< 0.01
21. Eurobank Ergasias services S.A	EES	Greece	−7.03E-05	0.039	0.916	13.872	< 0.01
22. National Bank of Greece SA	BK OF GR	Greece	9.12E-04	0.043	2.061	18.946	0.163
23. Piraeus Bank SA	PIR	Greece	2.42E-03	0.051	1.522	12.743	< 0.01
24. OTP Bank Nyrt	OTP	Hungary	−3.80E-04	0.022	1.566	18.825	< 0.01

Table 1 continued

Institution	Short name	Country	Mean	Dev.st	Skew	Kurt	P^D
25. AIB Group PLC	AIB	Ireland	3.71E-04	0.034	0.557	12.151	< 0.01
26. Bank of Ireland Group PLC	BK OF IR	Ireland	5.18E-05	0.029	0.691	7.400	< 0.01
27. Banco BPM SpA	BPM	Italy	2.80E-04	0.030	0.503	5.838	< 0.01
28. BPER Banca	BPER	Italy	1.10E-04	0.029	0.319	8.955	0.088
29. Intesa Sanpaolo SpA	INTESA	Italy	1.83E-05	0.021	1.398	18.186	0.101
30. Mediobanca Banca SpA	MEDIO	Italy	−1.47E-04	0.021	1.428	17.278	0.111
31. UniCredit SpA	UNICREDIT	Italy	−5.16E-05	0.027	0.448	9.185	0.101
32. UBS AG/London	UBS	Switzerland	−2.03E-04	0.018	0.411	7.026	0.079
33. Banco Bilbao Vizcaya Argentaria SA	BBVA	Spain	−1.15E-04	0.022	0.460	8.192	0.080
34. Banco de Sabadell SA	SABADELL	Spain	1.28E-04	0.028	0.305	7.941	0.055
35. Bankinter SA	BANKINTER	Spain	−1.17E-04	0.020	0.215	9.103	< 0.01
36. CaixaBank SA	CAIXA	Spain	−1.01E-04	0.022	0.437	6.925	0.084

Fig. 1 G_{MES} for the four windows. The arc opacities vary in proportion to the weights, with each weight representing the intensity of the impact of one bank on another: **a** 11/19/2015 to 12/31/2017, **b** 01/01/2018 to 02/15/2020, **c** 02/16/2020 to 01/31/2022 and **d** 02/01/2022 to 03/08/2024

ΔCoVaR using residuals from an ARMA(1,1)-GARCH(1,1).[2] Below we compare the two networks that display the most notable differences in density, namely G_{MES} and $G_{\Delta\text{CoVaR}_\text{W}}$, where the latter refers to the parametric ΔCoVaR using residuals of an ARMA(1,1)-GARCH(1,1). The network $G_{\Delta\text{CoVaR}_\text{W}}$ has two peculiarities that produce differences in the network structure.

$G_{\Delta\text{CoVaR}_\text{W}}$ differs from the MES-based network because it combines an ARMA(1,1)–GARCH(1,1) filtering step, which accounts for volatility clustering in returns, with SCAD-penalized quantile regression, which induces sparsity in the estimated dependence structure. A potential concern regarding the quantile-crossing

[2] The plots of networks built on the non-parametric ΔCoVaR applied directly to returns and the parametric ΔCoVaR using returns are available upon request.

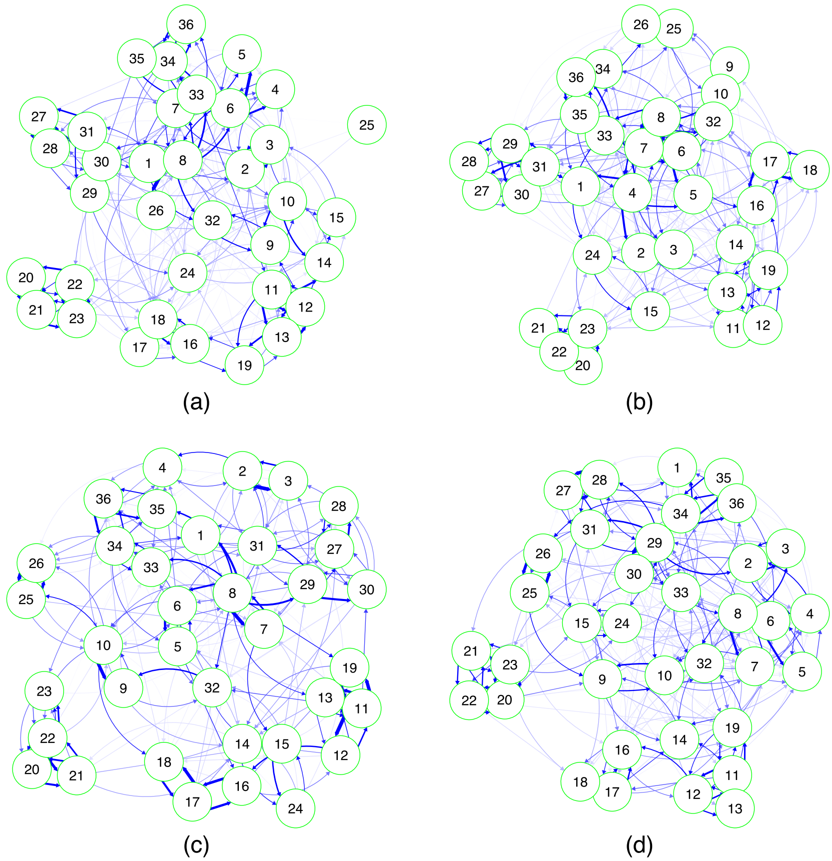

Fig. 2 $G_{\Delta\mathrm{CoVaR}_\mathrm{W}}$ (parametric ΔCoVaR using residuals of an ARMA(1,1)-GARCH(1,1)) for the four windows. The arc opacities vary in proportion to the weights, with each weight representing the intensity of the impact of one bank on another: **a** 11/19/2015 to 12/31/2017, **b** 01/01/2018 to 02/15/2020, **c** 02/16/2020 to 01/31/2022 and **d** 02/01/2022 to 03/08/2024

problem[3] is mitigated here by construction. In our empirical implementation, the dependence structure is estimated through a conditional median network, that is, a quantile graphical model evaluated only at the median level $\bar{\alpha} = 0.5$. The resulting coefficients are then used as the building blocks for the parametric residual-based ΔCoVaR specification. Under the Gaussian working specification adopted for the standardized ARMA(1,1)–GARCH(1,1) residuals, the slope coefficients of the conditional quantile function do not vary across probability levels, so the conditional median coefficients can be used to recover tail effects analytically. For this reason, the parametric specification is not obtained from separately estimated conditional quantiles across probability levels, and quantile crossing does not arise in this implementation.

[3] Quantile crossing refers to the violation of the monotonicity property of quantiles when they are estimated separately across probability levels, so that a lower conditional quantile may exceed a higher one; see, e.g., Aprea et al. (2024).

Table 2 Top five ranked banks for out-strength, authority and hub of networks based on ΔCoVaR of residuals and MES for the four time windows.

	I	II	III	IV
Out-strength				
ΔCoVaR	BNP	ING	BNP	INTESA
	ING	KBC	SK. VISCA	BNP
	CR. AGR	BNP	BARCL	SABADELL
	SK. VISCA	CR. AGR	SABADELL	SK. VISCA
	SV.HB	UNICREDIT	UNICREDIT	ALPHA
MES	ING	ING	CR. AGR.	ING
	BNP	CR. AGR.	BNP	BNP
	BANKINTER	BNP	BARCL	CR. AGR.
	CR. AGR.	BBVA	ING	KBC
	CAIXA	BANKINTER	BANKINTER	INTESA
Authority				
ΔCoVaR	BK OF IR	CR AGR	CR AGR	MEDIO
	CR AGR	BBVA	NORDEA	BBVA
	BBVA	BNP	COMMERZ	UNICREDIT
	INTESA	ING	SV.HB	ING
	ING	UBS	INTESA	NORDEA
MES	ING	ING	CR. AGR.	BNP
	BNP	CR. AGR.	BNP	ING
	BANKINTER	BNP	BARCL	CR. AGR.
	CR AGR	BBVA	ING	KBC
	BBVA	BANKINTER	ABN	INTESA
HUB				
ΔCoVaR	BNP	BNP	BNP	INTESA
	ING	ING	SK. VISCA	BNP
	UNICREDIT	KBC	SABADELL	SABADELL
	BANKINTER	CR AGR	UNICREDIT	BPER
	CR AGR	UNICREDIT	INTESA	SK. VISCA

4.1 Strength, hubs and authorities

In this section we focus on the scores that are related to risk diffusion in the two networks. In Table 2 we provide the top five ranked banks based on the scores of measures such as out-strength, authority and hub for the four time windows. As concerns the hub score, the main finding is that the persistence of BNP Paribas at the top of the hub ranking across time windows suggests a structurally central role in the propagation of tail risk, rather than a temporary prominence driven by short-term volatility conditions. Another interesting observation is that Bank of Ireland, in the network based on ΔCoVaR, turns out to be the authority with the highest rank for the first time window.

Table 3 Correlation and cosine similarity of ranks in networks based on MES produced using measures such *strength*, *authority*, *hub score* and *default probability*.

	strength_out_rank	auth_rank	hub_rank	P^D rank
Correlation				
strength_out_rank	1	0.851	0.999	0.296
auth_rank	0.851	1	0.859	0.189
hub_rank	0.999	0.859	1	0.274
P^D	0.296	0.189	0.274	1
Cosine similarity				
strength_out_rank	1	0.964	1.000	0.832
auth_rank	0.964	1	0.966	0.807
hub_rank	1.000	0.966	1	0.827
P^D	0.832	0.807	0.827	1

We use centrality and fragility rankings coupled with other bank specific quantities such as probability of default in order to highlight possible links between creditworthiness and risk propagation. Given two vectors w_1 and w_2, we compute the cosine similarity $S_C(w_1, w_2)$ as follows:

$$S_C(w_1, w_2) = \frac{\sum_{i=1}^{n} w_{1,i} w_{2,i}}{\sqrt{\sum_{i=1}^{n} w_{1,i}^2}\sqrt{\sum_{i=1}^{n} w_{2,i}^2}}. \tag{28}$$

This measure takes values in the interval $[-1, 1]$ where it is worth to describe three particular situations that correspond respectively to maximum dissimilarity $S_C(w_1, w_2) = -1$, orthogonality for $S_C(w_1, w_2) = 0$ and for $S_C(w_1, w_2) = 1$ perfect similarity. However, as our initial vectors contain positive elements being rankings based on measures such as strength, hub or authority introduced in Sect. 3, we get $S_C(w_1, w_2) \in [0, 1]$. We perform this analysis only for the last window as data for default probability refer to March 2024. We present in Tables 3 and 4 the correlation and the cosine similarity of vectors containing ranks in networks based respectively on ΔCoVaR and MES produced using measures such *strength*, *authority*, *hub score*, and *default probability*.

We provide a more detailed analysis of the relationship between network-based rankings and default probability (PD), with the aim of disentangling systemic interconnectedness from individual credit risk. The upper panels of Tables 3 and 4 show that Pearson correlations between PD ranks and network centrality ranks are generally weak or moderate. This indicates that systemic importance, as captured by network topology, does not coincide with individual credit risk. While PD reflects the standalone likelihood of default of a bank, network centrality measures capture the institution's position in the risk propagation structure, namely its ability to transmit or receive shocks within the system. The weak correlation therefore suggests that highly interconnected institutions are not necessarily those with the highest individual default

Table 4 Correlation and cosine similarity of ranks in networks based on ΔCoVaR produced using measures such *strength*, *authority*, *hub score* and *default probability*.

	strength_out_rank	auth_rank	hub_rank	P^D rank
Correlation				
strength_out_rank	1	0.236	0.803	−0.065
auth_rank	0.236	1	0.489	0.323
hub_rank	0.803	0.489	1	0.135
P^D	−0.065	0.323	0.135	1
Cosine similarity				
	strength_out_rank	auth_rank	hub_rank	P^D rank
strength_out_rank	1	0.817	0.953	0.746
auth_rank	0.817	1	0.877	0.839
hub_rank	0.953	0.877	1	0.794
P^D	0.746	0.839	0.794	1

probability, highlighting the conceptual distinction between systemic risk and individual credit risk. However, the lower panels of the same tables report cosine similarity values that are substantially higher. This apparent discrepancy stems from the different nature of the two similarity metrics. Correlation measures linear comovement between centered ranking vectors and is sensitive to systematic shifts in relative ordering. Cosine similarity, instead, evaluates the angular proximity between vectors and is invariant to common positive rescaling. As a result, cosine similarity captures the overall structural alignment between rankings, even when linear correlation is modest. The coexistence of weak Pearson correlations and relatively high cosine similarity implies that, although PD does not move proportionally with network centrality ranks, the overall ordering structure retains a degree of consistency. In economic terms, default probability partially overlaps with systemic relevance in terms of relative positioning, but does not fully explain the central role of institutions in the network. From a policy perspective, these findings imply that macroprudential surveillance frameworks should complement institution-specific solvency indicators with network-based systemic metrics. Monitoring centrality, clustering and community structures may provide early warning signals of contagion amplification mechanisms that are not directly observable through individual risk measures alone.

4.1.1 Clustering coefficient

We calculate for G_{MES} and $G_{\Delta\mathrm{CoVaR_W}}$ the local in- and out-clustering coefficients with both formulations proposed in Fagiolo (2007) and Clemente and Grassi (2018), within each window, in order to evaluate the interconnectedness of the system. We approach the role of banks in the financial system from two distinct angles by separately examining the in- and out-components. The in-clustering coefficient of a node i evaluates the impact of other banks' tail losses on the expected returns of bank i within the network. Conversely, the out-clustering coefficient focuses on how bank i's lower tail returns influence the expected returns of the other banks. These distinctive perspectives provide valuable insights into the interdependence of banks within the financial system. To this end, we investigate the behavior of individual banks based on the ranking of their clustering coefficients. We arrange the banks in decreasing order of their in- and out-clustering coefficients for each time window. Tables 5 and 6 display the top five ranked banks for this indicator for both variants of the systemic risk. As clustering captures the extent to which a bank is embedded in tightly interconnected local structures, high in-clustering values can be interpreted as indicators of greater exposure to contagion, whereas high out-clustering values point to a stronger role in local risk propagation. For the in-clustering coefficient we notice that $C_i^{\mathrm{F}\ in}$ and $C_i^{\mathrm{BCG}\ in}$ computed on the network $G_{\Delta\mathrm{CoVaR_W}}$ produce similar results in terms of the top five ranked banks. In particular, Greek banks and Scandinavian banks stand out in all the time windows, showcasing a notable trend wherein institutions from the same country tend to form tighter connections with each other compared to other banks in the system. This heightened interconnectedness may result in these banks experiencing correlated vulnerabilities and being more susceptible to common shocks or disruptions. The geographical proximity and shared national characteristics of the banks can contribute to this phenomenon, emphasizing the potential impact of regional dynamics on their collective resilience and susceptibility to systemic events. Surprisingly, in the third window, the Irish bank AIB has the highest value of the clustering coefficient with both formulations. Impact of tail losses of other banks seems to be diminishing for Swedish banks in recent periods. These results are not confirmed by the clustering coefficients computed on the network G_{MES}. $C_i^{\mathrm{F}\ in}$ identifies as the most exposed the banks of the central part of Europe (mainly in France, Netherlands and Spain) while the sets of banks designated by $C_i^{\mathrm{BCG}\ in}$ exhibit greater geographical diversification over time. The most striking result relates to the fact that unlike $C_i^{\mathrm{F}\ in}$, the coefficient $C_i^{\mathrm{BCG}\ in}$ identifies AIB as the bank with the highest in-clustering coefficient. For the out-clustering coefficients $C_i^{\mathrm{F}\ out}$ and $C_i^{\mathrm{BCG}\ out}$ for $G_{\Delta\mathrm{CoVaR}}$ give quite similar results in the first three windows. They both attribute an important role in the spread of the crisis mainly to Greek banks. The results for G_{MES} are still different for the two specifications of the clustering coefficients. $C_i^{\mathrm{F}\ out}$ assigns the most prominent role in risk diffusion to the French banks BNP Paribas and Crédit Agricole, while with $C_i^{\mathrm{BCG}\ out}$ we get different banks in each window. In the first window there are only Greek banks, in the second there are three Spanish banks, one Danish and one German. In the post-COVID period, risk seems to be propagated through banks in Central European countries.

4.1.2 Communities

We identify communities over time by implementing the Walktrap algorithm on both networks G_{MES} and $G_{\Delta\mathrm{CoVaR_W}}$. The composition pattern of the communities is displayed in Figs. 3 and 4.

Table 5 Top five ranked banks for the in- and out-clustering coefficients (Fagiolo) based on ΔCoVaR and MES for the four time windows.

	I	II	III	IV
In-clustering coefficients (Fagiolo)				
ΔCoVaR	SWED	EES	AIB	BANKINTER
	PIR	BK OF GR	ALPHA	ALPHA
	ALPHA	BPER	PIR	EES
	EES	SWED	EES	BK OF GR
	SV.HB	CAIXA	SV.HB	SV.HB
MES	ING	ING	CR. AGR	ING
	BANKINTER	CR. AGR	BNP	BNP
	BNP	BNP	BARCL	CR. AGR
	CR. AGR	BANKINTER	ING	KBC
	CAIXA	CAIXA	ABN	INTESA
Out-clustering coefficient (Fagiolo)				
ΔCoVaR	ALPHA	BPER	ALPHA	SV.HB
	EES	BPM	PIR	PIR
	MEDIO	ALPHA	AIB	EES
	BANKINTER	PIR	INTESA	BK OF GR
	BBVA	EES	BK OF GR	SK.VISCA
MES	BNP	BNP	BNP	BNP
	CR. AGR	CR. AGR	CR. AGR	INTESA
	SK VISCA	BBVA	ING	ING
	ING	KBC	INTESA	CR. AGR
	BANKINTER	ING	BARCL	NORDEA

Table 6 Top five ranked banks for in- and out-clustering coefficients (BCG) based on ΔCoVaR and MES for the four time windows.

	I	II	III	IV
In-clustering coefficient (BCG)				
ΔCoVaR	SWED	SWED	AIB	ALPHA
	ALPHA	EES	ALPHA	BANKINTER
	PIR	BK OF GR	PIR	BK OF GR
	SV.HB	BPER	OTP	EES
	EUROBANK	ALPHA	JYSKE	SV. HB
MES	PIR	EES	AIB	CR. AGR
	ALPHA	DANSKE	ERSTE	BNP
	AIB	SYD	KBC	SV. HB
	BK OF GR	INTESA	CR. AGR	SYD
	BPKO	UBS	HBSC	NORDEA
Out-clustering coefficient (BCG)				
ΔCoVaR	ALPHA	BPER	ALPHA	BK OF GR
	AIB	BK OF IR	OTP	ALPHA
	CAIXA	SV.HB	PIR	PIR
	MEDIO	ALPHA	AIB	RAIFF
	BPKO	PIR	BPM	OTP
MES	BK OF GR	SYD	AIB	JYSKE
	PIR	CAIXA	BPER	RAIFF
	AIB	SABADELL	COMMERZ	KBC
	ALPHA	COMMERZ	RAIFF	BNP
	EES	BANKINTER	ABN	BARCL

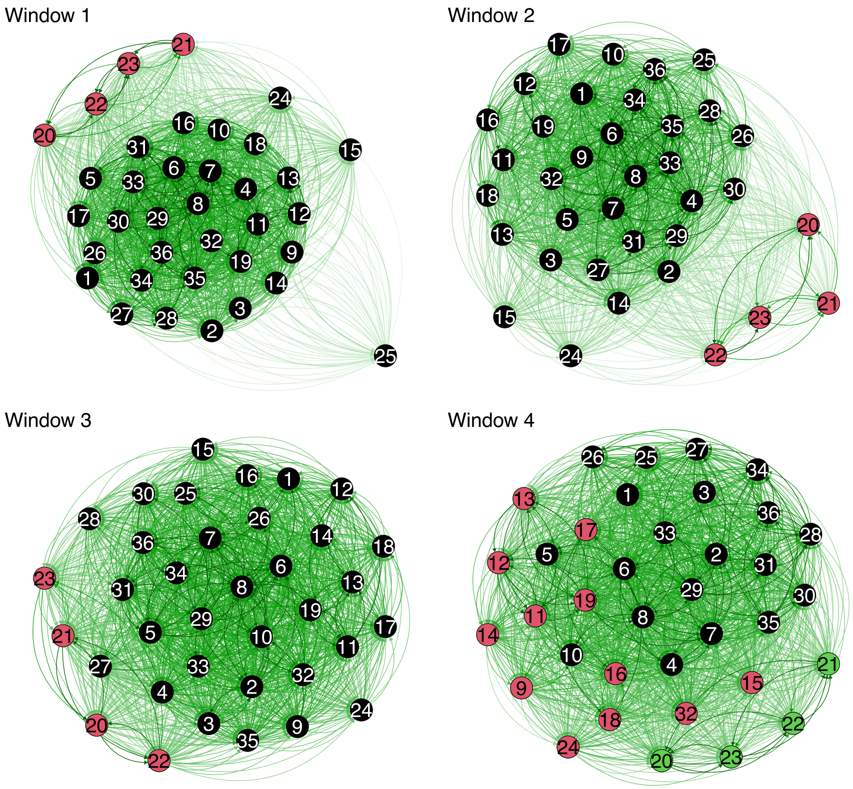

Fig. 3 Communities detected via Walktrap algorithm on network G_{MES} for each time window

According to Fig. 3, the MES-based network initially exhibits two communities in the first three time windows: a smaller group formed by the Greek banks and a larger group including the remaining institutions in the system. In the fourth window, the community structure evolves into three groups: one including Scandinavian banks together with Hungary and Switzerland, a second one involving banks from Italy, Austria, Germany, Belgium, the Netherlands, France, the UK, Ireland and Spain, and a third residual community formed by the Greek banks. This transition from two to three communities is consistent with a reconfiguration of systemic interdependencies over time. The repeated clustering of Greek banks across the four windows may reflect persistent similarities in their return dynamics and common macro-financial exposures, although sample composition may also contribute to this regularity.

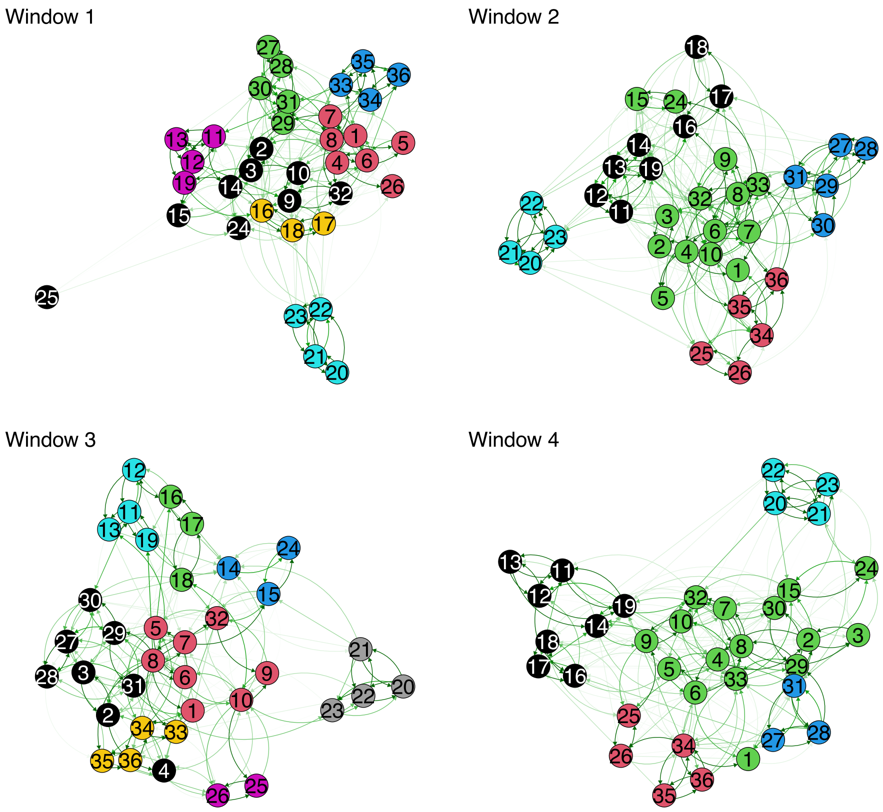

Fig. 4 Communities detected via Walktrap algorithm on network $G_{\Delta\mathrm{CoVaR_W}}$ for each time window

For $G_{\Delta\mathrm{CoVaR_W}}$, we detect seven communities in the first time window: the first is formed by Greek banks, the second by Sweden and Finland, the third by Italian banks, the fourth by Spanish banks, the fifth involves Germany, Belgium, the Netherlands, France and Ireland, the sixth groups the Danish banks, and the seventh includes Austria, Finland, Norway and Switzerland.

In the second window, the Walktrap algorithm detects five communities. This change in the number of communities is consistent with an evolution in the dependence structure across institutions. In this period, Italian banks continue to display a relatively cohesive grouping, while the Polish and Hungarian banks are included in the community involving Austria, Belgium and Germany. We also observe that the UK-related component becomes closer to the community of central European countries, a pattern that may be consistent with the gradual reorganization of cross-border banking linkages after the Brexit referendum.

The detection of eight communities in the third window suggests a further differentiation of the community structure during the COVID-19 crisis. This increase in the number of communities may indicate a more segmented dependence structure, with geographical proximity remaining an important organizing factor. The return to five communities in the fourth window points to a partial reorganization of the network during a period characterized by geopolitical uncertainty and high inflation in the euro area.

In particular, the banks operating in Sweden, Norway, Denmark and Finland form a single community, while the Polish bank remains within the group of central European countries. In the same window, Irish and Spanish banks appear again in close proximity, which may reflect the role of operational subsidiaries of UK banks in locations such as Dublin or Madrid. As far as Italian banks are concerned, for the first time we observe a separation into different communities. This configuration may also be consistent with contemporaneous market expectations regarding possible merger scenarios involving UniCredit, Banco BPM and BPER.

Overall, the varying number of communities across windows underscores the time-varying nature of the dependence structure captured by the ΔCoVaR network. The repeated grouping of Greek banks suggests a persistent pattern of similarity in their network position, although this result should be interpreted jointly with the composition of the empirical sample.

The differences in community composition across risk measures further reinforce the idea that alternative tail-risk metrics capture distinct layers of systemic interaction. MES-based communities tend to reflect stronger bilateral tail comovements, often producing larger and more cohesive clusters. In contrast, ΔCoVaR-based networks, relying on conditional quantile dependence structures, reveal more segmented and geographically differentiated communities, especially during periods of heightened macroeconomic uncertainty.

The time-varying community structure highlights that systemic risk propagation is shaped not only by individual bank characteristics, but also by evolving interaction patterns at the community level. The emergence, fragmentation and reconsolidation of communities across windows provide evidence that systemic relevance is jointly determined by macroeconomic conditions and endogenous network reconfiguration.

5 Conclusions

In this paper we conducted a thorough comparison of networks of banks constructed using different risk measures. Market-based risk measures inherently possess a forward-looking nature and consistently capture tail dependence from a systemic risk perspective. On the other hand, networks provide a representation of the entire banking system and facilitate the quantification of indicators that gauge centrality and interconnectedness, which are fundamental elements in addressing systemic risk. We computed several centrality measures, in particular we focused on out-strength, hub and authority, while also considering centrality and fragility rankings alongside another bank-specific quantity like probability of default. Our results show that the MES-based network and the parametric residual-based ΔCoVaR network lead to different topological configurations, centrality rankings, clustering patterns and community structures, confirming that alternative tail-risk measures capture distinct dimensions of systemic interdependence. Furthermore, we calculated time-varying clustering coefficients as indicators of interdependence of the network. By evaluating the impact of other banks' tail losses on the expected returns of individual banks and vice versa, we acquire a thorough understanding of the interconnectedness of banks within the financial system. This approach allows us to identify the most vulnerable institutions in terms of contagion. With respect to the relationship between network-based measures and default probability, our findings suggest that systemic interconnectedness and individual credit risk should be regarded as related but distinct dimensions of financial vulnerability. In particular, Pearson correlations are generally weak or moderate, whereas cosine similarity points to a partial alignment in the overall ranking structure. We finally conducted an analysis of the communities identified by the Walktrap algorithm. This analysis suggests, on one hand, a reconfiguration of systemic risk dynamics and interdependencies among banks over time, indicating shifts in interconnectedness and systemic importance due to the influence of geopolitical and economic events. On the other hand, persisting patterns related to geographical proximity have also been observed. More generally, the empirical evidence highlights that systemic relevance is time-varying and depends both on macro-financial conditions and on the endogenous reorganization of the network structure. These findings support the usefulness of complementing institution-specific risk indicators with network-based measures in macroprudential surveillance.

Appendix A Residual diagnostics for the ARMA(1, 1)–GARCH(1, 1) specification

Given the selected ARMA(1, 1)–GARCH(1, 1) specification, we compute standardized residuals for each bank and for each of the four time windows considered in the analysis. The standardized residuals are obtained by dividing the estimated innovations by the corresponding conditional standard deviations. Residual-diagnostic Tables 7, 8, 9 and 10 report, for each bank and window, the mean and standard deviation of the standardized residuals, together with the Ljung–Box p-values computed on both the standardized residuals and their squares. The former test is used to detect remaining linear serial correlation, while the latter provides evidence on residual dependence in the conditional variance.

Overall, the diagnostic results are satisfactory. In most bank-window combinations, the Ljung–Box (LB) tests do not reject the null hypothesis of no remaining serial correlation in the standardized residuals, nor in their squares. A few isolated rejections are observed, namely for KBC in Window (a) for the standardized residuals, and for BANKINTER in Window (a) and CAIXA in Window (d) for the squared standardized residuals. The results indicate that the selected ARMA(1, 1)–GARCH(1, 1) specification provides an adequate filtering of both linear dependence and volatility clustering for the vast majority of the series.

Table 7 Residual diagnostics for ARMA(1,1)-GARCH(1,1), Window (a) 11/19/2015 to 12/31/2017. Columns report the mean and standard deviation of standardized residuals and Ljung–Box p-values for residuals and squared residuals

Institution	Mean	SD	LB p-val res	LB p-val squared res
COMMERZ	−0.00694	1.00416	0.5635	0.8665
ERSTE	0.02395	1.00121	0.6354	0.8042
RAIFF	0.01911	0.99465	0.1628	0.9916
KBC	0.01023	1.02464	0.0371	0.8550
ABN	0.01376	0.99452	0.6101	0.9489
ING	0.02306	1.04174	0.6725	0.8438
CR AGR	0.00403	1.01685	0.5401	0.9996
BNP	−0.01839	1.02160	0.5051	0.9979
HSBC	0.01050	0.95251	0.8332	0.9158
BARCL	−0.01005	0.99821	0.5220	0.7867
SK.VISCA	0.00373	0.97025	0.6415	0.9985
SWED	0.02146	1.00057	0.2102	0.9975
SV.HB	−0.01538	0.99764	0.4626	0.4760
DNB	0.00730	0.99624	0.9460	0.8894
BPKO	0.00279	0.95221	0.4095	0.9891
DANSKE	0.01319	0.99759	0.2359	0.8376
JYSKE	0.01100	1.00144	0.4196	0.9575
SYD	0.00531	1.00146	0.7965	0.9182
NORDEA	0.03276	1.00173	0.1780	0.9705
ALPHA	0.02909	0.97278	0.2716	0.9489
EES	0.00501	0.97394	0.4258	0.9626
BK OF GR	0.06072	0.96561	0.6384	0.9932
PIR	0.07694	0.97744	0.5503	0.7613
OTP	0.02035	1.00366	0.4522	0.9000
AIB	0.01535	1.04030	0.2525	0.6428
BK OF IR	0.01508	1.03011	0.6934	0.7732
BPM	0.05577	1.03032	0.1231	0.7115
BPER	0.02761	1.01225	0.7841	0.6109
INTESA	0.02129	1.06457	0.6675	0.5373
MEDIO	0.01422	1.04949	0.3868	0.8805
UNICREDIT	0.02097	1.01727	0.9486	0.6051
UBS	0.01448	0.99218	0.9866	0.9638
BBVA	0.00678	1.00353	0.7070	0.9957
SABADELL	−0.01603	1.00799	0.2196	0.9983
BANKINTER	0.00664	1.00351	0.6992	0.0122
CAIXA	−0.05186	1.00517	0.5416	0.2371

Table 8 Residual diagnostics for ARMA(1,1)-GARCH(1,1), Window (b) 01/01/2018 to 02/15/2020. Columns report the mean and standard deviation of standardized residuals and Ljung–Box p-values for residuals and squared residuals

Institution	Mean	SD	LB p-val res	LB p-val squared res
COMMERZ	0.00097	1.01051	0.8721	0.4047
ERSTE	0.01074	0.99778	0.7996	0.5607
RAIFF	0.00571	0.97313	0.9388	0.8787
KBC	0.00399	1.00249	0.9360	0.9954
ABN	−0.00729	1.00348	0.3053	1.0000
ING	0.00217	1.01135	0.7820	0.5574
CR AGR	0.00507	0.99836	0.9410	0.3015
BNP	0.00436	1.00843	0.9754	0.8761
HSBC	0.00064	1.00117	0.6973	0.7361
BARCL	−0.00729	1.00193	0.5879	0.7735
SK.VISCA	0.00066	1.00180	0.7369	0.9501
SWED	0.00674	1.00384	0.9533	0.8094
SV.HB	−0.01029	1.00141	0.4831	0.9932
DNB	0.00794	1.00177	0.5926	0.9921
BPKO	0.00091	1.00247	0.5348	0.3849
DANSKE	0.00288	1.01673	0.6433	0.9029
JYSKE	−0.00105	1.00383	0.7033	0.9957
SYD	0.00012	1.00192	0.1104	0.9992
NORDEA	0.00381	1.00244	0.5768	0.9029
ALPHA	0.01439	1.03199	0.0831	0.4796
EES	0.02084	1.00631	0.3683	0.4529
BK OF GR	0.00347	1.02279	0.1297	0.9976
PIR	0.01785	1.01459	0.4692	0.5209
OTP	0.00720	0.99870	0.8504	0.0892
AIB	−0.00252	1.01488	0.5970	0.8580
BK OF IR	0.01059	1.00383	0.6809	0.3911
BPM	0.00662	1.00160	0.9666	0.9886
BPER	0.01383	1.00244	0.8265	0.8055
INTESA	0.04743	1.00034	0.6537	0.9995
MEDIO	0.02786	1.01275	0.5351	0.7258
UNICREDIT	0.00994	1.00437	0.5064	0.6739
UBS	0.00903	1.00196	0.9479	0.5062
BBVA	0.00220	1.00580	0.9922	0.5505
SABADELL	0.00172	1.00344	0.4503	0.9972
BANKINTER	−0.00052	1.00299	0.8081	0.9666
CAIXA	0.00328	1.00519	0.9607	0.4665

Table 9 Residual diagnostics for ARMA(1,1)-GARCH(1,1), Window (c) 02/16/2020 to 01/31/2022. Columns report the mean and standard deviation of standardized residuals and Ljung–Box p-values for residuals and squared residuals

Institution	Mean	SD	LB p-val res	LB p-val squared res
COMMERZ	0.01526	0.99570	0.2016	0.7394
ERSTE	0.04365	0.99097	0.1130	0.9758
RAIFF	0.01976	0.99593	0.5557	0.9866
KBC	0.02053	0.94239	0.9320	0.9186
ABN	0.02013	0.93123	0.9592	0.9636
ING	0.03246	0.95822	0.9573	0.4328
CR AGR	0.02328	0.95611	0.9021	0.8870
BNP	0.03294	0.96760	0.7580	0.9671
HSBC	0.00452	0.95328	0.7224	0.9275
BARCL	0.01043	0.95230	0.6401	0.9558
SK.VISCA	0.03948	0.99305	0.6826	0.9180
SWED	0.00664	0.93540	0.8435	0.9295
SV.HB	−0.00627	0.94026	0.5841	0.9968
DNB	0.03367	1.00095	0.9131	0.9806
BPKO	0.05199	0.99168	0.7477	0.6647
DANSKE	0.00202	0.95616	0.8956	0.9978
JYSKE	0.01309	0.98616	0.8320	0.1236
SYD	−0.00045	1.00449	0.2073	0.8490
NORDEA	0.02653	0.95594	0.9321	0.9015
ALPHA	0.06565	0.99692	0.3183	1.0000
EES	0.03762	0.96412	0.8323	0.9908
BK OF GR	0.03587	0.99036	0.4661	0.9912
PIR	0.10179	1.03501	0.2614	0.9688
OTP	0.03128	0.99432	0.9733	0.6522
AIB	0.05033	0.99913	0.4666	0.3555
BK OF IR	0.02655	0.93900	0.6992	0.8575
BPM	0.03794	0.94827	0.6502	0.9845
BPER	0.03007	0.94416	0.6586	0.9789
INTESA	0.06042	0.97416	0.5357	0.6064
MEDIO	0.02622	0.96646	0.4362	0.6607
UNICREDIT	0.03891	0.99387	0.2988	0.2634
UBS	0.04294	0.99029	0.7823	0.8728
BBVA	0.05050	1.00159	0.5847	0.3859
SABADELL	0.02673	1.00215	0.5249	0.1028
BANKINTER	0.02796	0.97889	0.5356	0.9344
CAIXA	0.02274	0.95176	0.9475	0.7948

Table 10 Residual diagnostics for ARMA(1,1)-GARCH(1,1), Window (d) 02/01/2022 to 03/08/2024. Columns report the mean and standard deviation of standardized residuals and Ljung–Box p-values for residuals and squared residuals

Institution	Mean	SD	LB p-val res	LB p-val squared res
COMMERZ	0.01029	1.00036	0.4576	0.9841
ERSTE	0.03897	0.95979	0.9494	0.9983
RAIFF	0.02782	0.99951	0.5418	0.9986
KBC	0.05747	1.00150	0.8341	0.7187
ABN	0.00213	0.93414	0.8413	0.8875
ING	0.03650	0.99765	0.9701	0.9905
CR AGR	0.01298	0.95949	0.8776	0.9982
BNP	0.03559	1.00171	0.9386	0.9819
HSBC	0.01409	1.00169	0.4511	0.9854
BARCL	0.03137	1.00172	0.5256	0.9702
SK.VISCA	0.02076	0.97796	0.6528	0.6821
SWED	0.01519	0.96003	0.5266	0.9304
SV.HB	0.01205	1.00064	0.9649	0.8452
DNB	0.00666	0.99289	0.3417	0.9709
BPKO	0.03373	0.99582	0.2833	0.9082
DANSKE	0.02129	1.00093	0.2786	0.9999
JYSKE	0.00673	0.97162	0.5061	0.1500
SYD	0.02096	0.98732	0.9035	0.8007
NORDEA	0.03575	1.00195	0.7347	0.3800
ALPHA	0.03667	0.99932	0.7490	0.9726
EES	0.02891	0.96990	0.0880	0.6964
BK OF GR	0.03017	1.00206	0.7622	0.9178
PIR	0.02406	0.99527	0.7581	0.9928
OTP	0.09491	1.00387	0.1435	0.9926
AIB	0.03161	0.99907	0.7318	0.9594
BK OF IR	−0.02849	1.00207	0.4176	0.8390
BPM	0.02496	0.99198	0.7410	0.9855
BPER	0.04229	1.00188	0.8259	0.9886
INTESA	0.05213	1.00056	0.8260	0.9992
MEDIO	0.03515	1.00046	0.8863	0.8700
UNICREDIT	0.03688	0.98096	0.5762	0.9316
UBS	0.02366	1.00187	0.8992	0.8582
BBVA	0.04750	0.99896	0.8779	0.9392
SABADELL	0.02816	0.99726	0.8168	0.9674
BANKINTER	0.01383	1.00015	0.4993	0.5897
CAIXA	−0.01051	0.96730	0.1929	0.0372

Funding Open access funding provided by Università degli Studi di Milano - Bicocca within the CRUI-CARE Agreement. This work was supported by the Italian Ministry of University and Research (Ministero dell'Università e della Ricerca, MUR). Prof. Alessandra Cornaro was supported under project 2022LT8P4J (CUP: H53D23002510006).
Prof. Edit Rroji and PhD. Ilaria Stefani were supported under project 20225PC98R (CUP: H53D23002200006).

Declarations

Conflict of interest The author declares that there are no conflict of interest.

References

Kleinow, J., Moreira, F.: Systemic risk among European banks: A copula approach. J. Int. Finan. Markets. Inst. Money **42**, 27–42 (2016)

Magner, N., Lavin, J.F., Valle, M., Hardy, N.: The predictive power of stock market's expectations volatility: A financial synchronization phenomenon. PLoS ONE **16**(5), 0250846 (2021)

Adrian, T., Brunnermeier, M.K.: CoVaR. Am. Econ. Rev. **106**(7), 1705 (2016)

López-Espinosa, G., Moreno, A., Rubia, A., Valderrama, L.: Short-term wholesale funding and systemic risk: A global CoVaR approach. J. Bank. Finance **36**(12), 3150–3162 (2012)

Pellegrini, C.B., Cincinelli, P., Meoli, M., Urga, G.: The role of shadow banking in systemic risk in the European financial system. J. Bank. Finance **138**, 106422 (2022)

Xu, Q., Li, M., Jiang, C., He, Y.: Interconnectedness and systemic risk network of chinese financial institutions: A LASSO-CoVaR approach. Physica A **534**, 122173 (2019)

Ali, A., Kolter, J.Z., Tibshirani, R.J.: The multiple quantile graphical model. Adv. Neural. Inf. Process. Syst. **29**, 3747–3755 (2016)

Belloni, A., Chen, M., Chernozhukov, V.: Quantile graphical models: Prediction and conditional independence with applications to financial risk management (2016). (Working paper)

Torri, G., Giacometti, R., Tichỳ, T.: Network tail risk estimation in the European banking system. J. Econ. Dyn. Control **127**, 104125 (2021)

Aprea, I.L., Scognamiglio, S., Zanetti, P.: Systemic risk measurement: A Quantile Long Short-Term Memory network approach. Appl. Soft Comput. **152**, 111224 (2024)

Fiori, A.M., Porro, F.: A compositional analysis of systemic risk in European financial institutions. Ann. Finance **19**(3), 325–354 (2023)

Clemente, G.P., Grassi, R., Pederzoli, C.: Networks and market-based measures of systemic risk: the European banking system in the aftermath of the financial crisis. J. Econ. Interac. Coord. **15**(1), 159–181 (2020)

Acharya, V.V., Pedersen, L.H., Philippon, T., Richardson, M.: Measuring systemic risk. Rev. Financial Stud. **30**(1), 2–47 (2017)

Clemente, G.P., Cornaro, A.: A multilayer approach for systemic risk in the insurance sector. Chaos, Solitons Fractals **162**, 112398 (2022)

Idier, J., Lamé, G., Mésonnier, J.: How useful is the marginal expected shortfall for the measurement of systemic exposure? A practical assessment. J. Bank. Finance **47**, 134–146 (2014)

Abduraimova, K.: Contagion and tail risk in complex financial networks. J.Bank. Finance **143**, 106560 (2022)

Brownlees, C., Engle, R.F.: SRISK: A conditional capital shortfall measure of systemic risk. Rev. Financial Stud. **30**(1), 48–79 (2017)
Hautsch, N., Schaumburg, J., Schienle, M.: Financial network systemic risk contributions. Rev. Finance **19**(2), 685–738 (2015)
Bellini, F., Mercuri, L., Rroji, E.: On the dependence structure between S&P500, VIX and implicit Interexpectile Differences. Quantitative Finance **20**(11), 1839–1848 (2020)
Benoit, S., Colliard, J.E., Hurlin, C., Pérignon, C.: Where the risks lie: A survey on systemic risk. Rev. Finance **21**(1), 109–152 (2016)
Koenker, R., G., B.J.: Regression quantiles. Econometrica: journal of the Econometric Society, pp. 33–50 (1978)
Wu, Y., Liu, Y.: Variable selection in quantile regression. Stat. Sin. pp. 801–817 (2009)
Fan, J., Li, R.: Variable selection via nonconcave penalized likelihood and its oracle properties. J. Am. Stat. Assoc. **96**(456), 1348–1360 (2001)
Bang-Jensen, J., Gutin, G.Z.: Digraphs: Theory, Algorithms and Applications, 2nd edn. Springer, London, UK (2009)
Harary, F.: Graph Theory. Addison-Wesley Publishing Company, Reading, Mass (1969)
Horn, R.A., Johnson, C.R.: Matrix Analysis, 2nd edn. Cambridge University Press, New York, NY, USA (2012)
Kleinberg, J.M.: Authoritative sources in a hyperlinked environment. J. ACM (JACM) **46**(5), 604–632 (1999)
Kleinberg, J.M.: Hubs, authorities, and communities. ACM Computing Surv. (CSUR) **31**(4es), 5 (1999)
Fagiolo, G.: Clustering in complex directed networks. Phys. Rev. E **76**(2), 026107 (2007)
Clemente, G.P., Grassi, R.: Directed clustering in weighted networks: A new perspective. Chaos, Solitons Fractals **107**, 26–38 (2018)
Pons, P., Latapy, M.: Computing communities in large networks using random walks. J. Graph Algorithms Appl. **10**(2), 191–218 (2006)